

Adaptive Assist-As-Needed Controller to Improve Gait Symmetry in Robot-Assisted Gait Training

Damiano Zanotto, Paul Stegall, Sunil K. Agrawal*,
Robotics and Rehabilitation (ROAR) Laboratory, Columbia University, New York, NY 10027
{dz2265, prs2136, sunil.agrawal}@columbia.edu

*Corresponding Author

Abstract—This paper introduces the overall design of ALEX III, the third generation of Active Leg Exoskeletons developed by our group. ALEX III is the first treadmill-based rehabilitation robot featuring 12 actively controlled degrees of freedom (DOF): 4 at the pelvis and 4 at each leg. As a first application of the device, we present an adaptive controller aimed to improve gait symmetry in hemiparetic subjects. The controller continuously modulates the assistive force applied to the impaired leg, based on the outputs of kernel-based non-linear filters, which learn the movements of the healthy leg. To test the effectiveness of the controller, we induced asymmetry in the gait of three young healthy subjects adding ankle weights (2.3kg). Results on kinematic data showed that gait symmetry was recovered when the controller was active.

I. INTRODUCTION

Stroke often results in a combination of cognitive, sensory and motor impairments [1]. The most common movement impairment following stroke is hemiparesis, a condition that encompasses weakness and reduced motor function on one side of the body, and may involve facial muscles as well as the upper and lower extremities [2], [3].

Affected subjects may experience difficulties in performing basic activities of daily living, such as eating, dressing, handling objects, etc. Even though stroke survivors are usually ambulatory [4], their walking capacity is limited and requires repetitive task-specific training [5] and intense physiotherapy [6] for recovery. Typical features of impaired gait function are reduced walking speed, endurance, joints ranges of motion, and spatial and temporal symmetry. Gait asymmetry, in particular, is thought to be mainly correlated to the degree of spasticity of the affected ankle plantarflexors [7]. Several symmetry ratios might be utilized to quantify gait asymmetry [8]. Post-stroke subjects, for instance, might show step-length ratios (affected limb over unaffected limb) of approximately 1.13, and single-support ratios ranging from 0.53 to 0.66 [7].

The rationale behind robot-aided gait rehabilitation is that robotic devices have the potential to reduce the physical burden on the therapists and the costs of treatments, as well as to increase the duration and frequency of the training sessions, while allowing for continuous, quantitative assessment of the level of motor function recovery [9]. However, after more than ten years since early robotic gait trainers were first proposed [10], there is still no consensus about the superiority of this technology compared to traditional forms of physiotherapy [11]. The lack of clear results further challenge the robotics

community to develop novel design solutions and control strategies that better support motor re-learning [12], [9].

Early robot trainers actively controlled hip and knee joint motions only. This approach, however, may induce compensatory strategies on the subjects rather than helping them develop a normal gait [13]. Indeed, the pelvis and the ankle play a key role in walking: the former facilitates swing and load shifting between legs [14], [15], the latter contribute to trunk support, forward progression and swing initiation [16].

This paper deals with ALEX III, the first treadmill-based bilateral exoskeleton capable of applying controlled forces to the pelvis, hip, knee and ankle joints at the same time. The device is the third prototype of Active Leg Exoskeleton (ALEX) developed by our research group [17], [18], and was designed to actively control 4-DOF at each leg (hip adduction/abduction, hip and knee flexion/extension, ankle plantar/dorsiflexion), as well as 4-DOF at the pelvis (vertical rotation, anterior/posterior, superior/inferior and lateral motions). These new features involved major design changes compared to previous versions of ALEX, which were unilateral devices, with hip and knee flexion/extension as the only active DOFs (pelvic motion was provided passively, ALEX II having the same pelvic DOFs as those of ALEX III, and ALEX I lacking anterior/posterior translation).

The focus of this paper is twofold: We first introduce the overall design of ALEX III, including the 4-DOF platform, and then illustrate a first application of the robot, where an adaptive controller is implemented to facilitate recovery of gait symmetry in impaired subjects. The controller integrates our previous implementation of the assist-as-needed paradigm (AAN), which consisted of a static non-linear force tunnel built around the target footpath [17], with novel adaptive capabilities provided by a pool of kernel-based nonlinear filters. These filters are synchronized to the phase of the gait, as estimated by adaptive frequency oscillators (AFO) [19], and they continuously modulate the force-field acting on the impaired leg by learning the trajectory of the healthy leg.

The use of adaptive frequency oscillators in combination with non-linear filters was first proposed in [20] in the context of supervised learning of periodic trajectories for humanoid robots. Only recently, however, AFO-based controllers have been applied to gait exoskeletons to reduce muscle effort in the wearer [21], [22] and to improve transparency [23]. *Here, we explore a novel application of this tool to an adaptive AAN controller aimed to facilitate recovery of gait*



Fig. 1: Subject walking in ALEX III with weights attached to his left distal shank.

symmetry. Feasibility of our approach is validated by means of experimental tests on a small group of healthy subjects.

II. ALEX III DESIGN

ALEX III is a bilateral exoskeleton, featuring a 4-DOF platform and two 4-DOF legs. Its design was conceptualized starting from two key-concepts: *flexibility* and *transparency*. With flexibility, we mean the possibility to test a wide set of training strategies (e.g., constrain some DOFs while providing variable assistive/perturbing forces to others). This was addressed by actively controlling those DOF that are most important in walking, and by appropriately choosing the size of the motors, such that the range of torques the robot can apply at a certain joint approximately matches the equivalent torques provided by human muscles around the same joint. To improve transparency, the mechanical impedance of the leg was minimized by mounting the actuators on the support platform, and by using a combination of rigid parallelogram linkages and loops of timing belts to remotely apply forces to the human lower limbs. *As a consequence, most of the mechanical components are located behind the wearer's legs, so that the subject can freely swing his/her arms while walking* (Fig. 1). In the following, we provide details on the design of the support platform, while a detailed description of the leg can be found in [24].

The vertical and anterior/posterior motions of the support platform are enabled by four legs. The rear legs consist of a parallel linkage, with Cardan universal joints at the top and the bottom (Fig. 2). Due to the nature of the parallel linkages, each rear leg is equivalent to a *virtual leg* that runs parallel to the rear leg and passes through the top of the front leg. The top of the each leg is independently capable of reaching a spherical shell. By connecting the top of the front and virtual legs together - as it is done on the left and right sides of the platform - the reachable space is restricted to the intersection

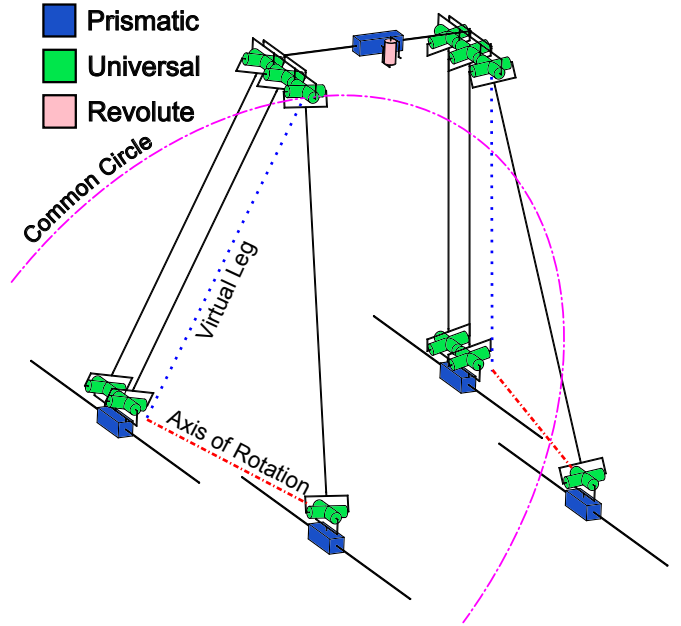


Fig. 2: Kinematic diagram of the support system.

of the front and virtual legs' shells, i.e. a *common circle*. The latter lies in the radical plane of the two spheres, with its center lying on the axis that connects the bases of the two legs (*axis of rotation* in Fig. 2), and its radius being the height of the triangle formed by the same axis and the two legs.

The left and right sides of the platform are connected to each other with rails. If the radical planes of both sides are the same, then the structure would behave like a four bar linkage in that plane. However, by moving the front prismatic joints closer together, distinct radical planes are created, thereby fixing the structure for any given position of the lower prismatic joints. The system can then be modeled as a PRRRP kinematic chain composed of the projection of the spatial chain onto the sagittal plane. Moving all the lower prismatic joints forward or backwards creates anterior and posterior motion, respectively. Increasing or decreasing the distance between the front and rear bases produces inferior and superior motion, respectively. On the rails connecting the left and right side of the platform rides a prismatic joint that produces lateral motion of the pelvis. This also carries a revolute joint providing rotation about the vertical axis. The exoskeletal legs and the wearer's belt are attached after this joint.

An alternative design solution would be to use two planar PRRRP kinematic chains, as proposed in [25], [26]. However, universal joints have a significant advantage. The moment arm created by the length of the support legs is substantial: if the joints were a single revolute joint, any lateral loading at the top of the support system would result in an extremely large moment at the base of each support leg. Conversely, by using universal joints, the ends of the support legs only see moments about the longitudinal axis of the leg, so they act mainly in compression. This allows for the use of smaller components, reducing mass and moment of inertia. The support legs

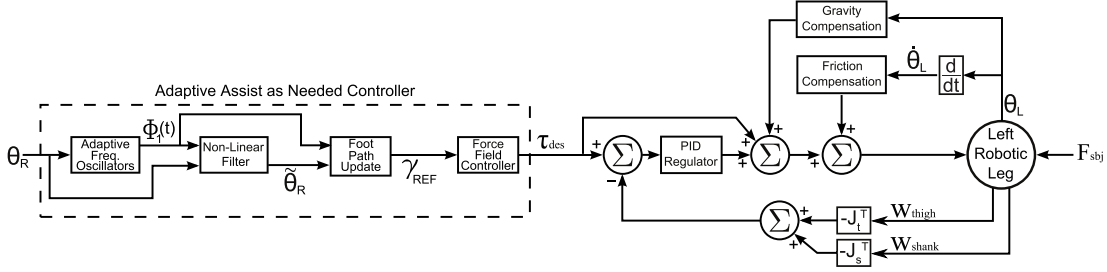


Fig. 3: Left leg control scheme

themselves are angled inward to help take lateral loading and increase stability.

III. ADAPTIVE AAN CONTROLLER

The low level controller of ALEX III is similar for the legs and the support platform. It consists of force feedback loops with gravity and friction compensation terms (Fig. 3, right side). Instead of controlling the actuators torque output (*traditional torque control*), we control the interaction error by closing the loop on force-torque sensors mounted between each robot orthosis and the user's body (*direct force control*). This approach was tested on an earlier version of ALEX [27] and proved to be effective in canceling out a significant fraction of the undesired interaction forces arising from the inertia of the robotic links, without the use of inertial compensators.

This section deals with an adaptive AAN controller aimed to facilitate recovery of gait symmetry. It integrates our previous implementation of the AAN paradigm (i.e., a static non-linear force tunnel built around the target footpath [17]), with novel adaptive capabilities provided by the combined use of adaptive oscillators and kernel-based nonlinear filters. The AFO is responsible to extract the phase of the gait, whereas non-linear filters learn the trajectories of the hip and knee joints of the unimpaired leg as a function of the phase. These are then utilized to continuously update a reference footpath, which shape the behavior of the assistive force field acting on the contralateral leg (Fig. 3, left side).

The joint angle trajectory $\theta(t)$ during walking can be approximated by a periodic non-sinusoidal signal, whose frequency spectrum comprises only multiples of a fundamental frequency. A suitable estimator $\hat{\theta}(t)$ can therefore be written as the sum of M oscillators [21]:

$$\hat{\theta}(t) = \theta_0 + \sum_{i=1}^M a_i \sin(\varphi_i(t)), \quad (1)$$

where the i -th oscillator tracks the i -th harmonic component, similarly to a real-time Fourier decomposition. We further assume that the phase of the fundamental harmonic, namely $\varphi_1(t)$, yields a good estimate of the gait phase. The set of equations governing how the pool of oscillators learns the frequency of the teaching signal $F(t) = \theta(t) - \hat{\theta}(t)$ is given by [21]:

$$\begin{aligned} \dot{\varphi}_i(t) &= i\omega + \varepsilon F(t) \cos(\varphi_i(t)), \quad i = 1, \dots, M \\ \dot{\omega}(t) &= \varepsilon F(t) \cos(\varphi_1(t)), \\ \dot{a}_i(t) &= \nu F(t) \sin(\varphi_i(t)), \quad i = 1, \dots, M \\ \dot{\theta}_0(t) &= \nu F(t), \end{aligned} \quad (2)$$

where φ_i , $(i\omega)$ are the phase and frequency of the i -th oscillator, and ε , ν are the coupling strength and the learning factor of the AFO.

Subsequently, based on the estimate $\varphi_1(t)$, N equally spaced kernel functions in the form $\Psi_i(\varphi_1(t)) = \exp[h(\cos(\varphi_1(t) - \frac{2\pi i}{N}) - 1)]$ are used to reconstruct the signal $\theta(t)$:

$$\tilde{\theta}(t) = \frac{\sum_{i=1}^N \Psi_i(\varphi_1(t)) w_i(t)}{\sum_{i=1}^N w_i(\varphi_1(t))} \quad (3)$$

Here, $\tilde{\theta}(t)$ is the reconstructed signal and h defines the width of the kernel functions. Incremental learning of weights w_i is achieved at each time sample n through a RLS method with forgetting factor λ [20]:

$$\begin{aligned} w_i(n+1) &= w_i(n) + \Psi_i(n) P_i(n+1) e_r(n), \\ e_r(n) &= [\theta(n) - w_i(n)], \\ P_i(n+1) &= \frac{1}{\lambda} \left(P_i(n) - \frac{P_i(n)^2}{\frac{\lambda}{\Psi_i(\varphi_1(n))} + P_i(n)} \right) \end{aligned} \quad (4)$$

This algorithm runs in parallel for the hip and knee flexion/extension angles of the unimpaired leg - as measured by the encoders embedded in the robot - yielding the estimates $\tilde{\theta}_{HIP}(t)$ and $\tilde{\theta}_{KNEE}(t)$. The parameter λ controls how quickly these estimates adapt to variations of the user's gait. If $\lambda=1$, the same relative importance is given to recent and older data, and therefore the algorithm adapts slowly. Conversely, when $\lambda < 1$, more importance is given to recent data, and the estimates adapt quickly.

Let $\gamma_{REF}(\varphi)$ be the target footpath for the impaired leg:

$$\gamma_{REF}(\varphi) = (x(\varphi), y(\varphi)), \quad \varphi \in [0; 2\pi], \quad (5)$$

then the most recent angle estimates, together with the information on the current phase, can be used to locally update the target footpath:

$$\gamma_{REF}(\varphi(t)) = f(\tilde{\theta}_{HIP}(t), \tilde{\theta}_{KNEE}(t)) \quad (6)$$

where f is the (forward kinematics) function mapping subject's hip and knee angles to the position of his/her foot in the sagittal plane. In (6), $\varphi(t)$ can be equivalently chosen as $\varphi_{1,HIP}(t)$ or $\varphi_{1,KNEE}(t)$. The assistive force to be exerted on the wearer's impaired foot depends on the position of the latter relative to γ_{REF} . The force-field behavior is modeled by a nonlinear virtual spring that exerts a normal force towards

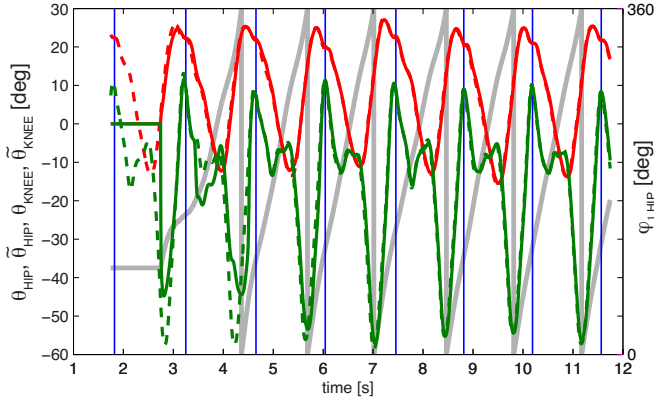


Fig. 4: Hip (red) and knee (green) angles of the right leg, as measured by encoders (dashed) and estimated by the non-linear filters (solid). Blue vertical lines and gray line indicate heel strikes and the phase estimate $\varphi_{1,HIP}$ respectively.

the prescribed footpath if the deviation of the subject's foot from γ_{REF} exceeds an adjustable threshold:

$$\mathbf{F} = \begin{cases} k_N(d - D_0)^2 \mathbf{n} & \text{if } (d > D_0), \\ 0 \mathbf{n} & \text{otherwise,} \end{cases} \quad (7)$$

where k_N is the stiffness of the virtual spring, D_0 is the width of the force tunnel, d is the distance of the subject's foot from γ_{REF} and \mathbf{n} is the unit vector directed along the line connecting the subject's ankle point to the closest point of γ_{REF} . \mathbf{F} is finally mapped to the vector of equivalent interaction torques τ_{des} which is fed to the low-level controller (Fig. 3).

In the ALEX III controller, AFO, non linear filters and footpath update run at 500Hz, whereas the force-field controller run at 1kHz. Preliminary tests showed that $M = 6$ oscillators with $\nu = 0.5$ and $\varepsilon = 12$ reach synchronization in about 3 steps. $N = 90$ was found to be a good tradeoff between accuracy of estimation and computational load, and the width of kernel functions was set to $h = 2.5N$. The forgetting factor $\lambda = 0.995$ was chosen experimentally to guarantee smooth adaptation of the reference footpath. Fig. 4 shows how $\varphi_{1,HIP}(t)$ and the estimates $\hat{\theta}_{HIP}(t)$ and $\hat{\theta}_{KNEE}(t)$ evolved with time, after the AFO was activated, at $t = 2.7s$, while a subject was walking in ALEX III at 0.9m/s. The AFO progressively synchronizes to the gait cycle and the nonlinear filters (anchored to the phase estimate) rapidly learn the input signals, such that estimation errors become negligible after 5 steps. Fig. 5 shows how the target footpath adapted as the treadmill speed was reduced from 1.0 to 0.5m/s.

One might argue that a simpler way of assisting gait symmetry would be to directly feed the trajectory of the unimpaired foot to reshape the force field. However, this approach might jeopardize gait stability in case of variations of the gait pattern induced, for instance, by changes of walking cadence. Indeed, the update of the reference template would be necessarily done all at once at discrete gait events (e.g., at initial contact of one foot). Conversely, with the approach proposed above the target footpath adapts smoothly to changes in frequency and shape:

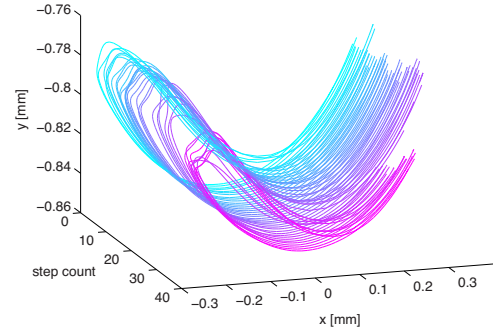


Fig. 5: Change in the reference footpath as the treadmill speed is reduced from 1.0 to 0.5m/s between steps 26 and 27.

the online estimation of the gait phase by means of the AFO allows for continuous update of the reference trajectory, while the action of non-linear filters with forgetting factor smoothens the transitions in gait footpath, thus preventing abrupt changes. The user is never constrained to follow a fixed trajectory and assistive forces are nil if his/her foot is sufficiently close to the reference footpath.

IV. EXPERIMENTAL VALIDATION

A. Protocol and data analysis

Three healthy male adults (age 29 ± 5 years, height $1.77 \pm 0.03m$, weight $70.3 \pm 2.1kg$) from our research group volunteered for this experiment, designed as an initial proof of concept validation of ALEX III and the adaptive AAN controller. To approximately mimic the asymmetric limb movement patterns associated with hemiparetic locomotion, we applied additional weight (2.3kg) to subject's left distal shank, and regarded the left leg as the "impaired" one. Location and magnitude of the load were chosen such as to alter gait kinematics significantly [28]. A 5-minute familiarization session was included prior to the experiment to let participants get used to walking in the exoskeleton. Afterwards, subjects walked in the robot under four different conditions, each one lasting 2 minutes, while the treadmill speed was set to 0.9m/s. In this experiment, pelvis rotation and lateral motion were locked in the robot, and the human ankle was not interfaced to the exoskeleton, to allow fitting of the ankle weight.

The first session (*baseline*) included treadmill walking while the robot was controlled in *zero-interaction mode*: the desired interaction torques reflected at the hip and knee joints of each leg were set to zero (i.e., $\tau_{des} = 0\mathbf{N}$ in Fig. 3), as were the desired interaction forces at the pelvic brace. This session was used to assess the subject's level of gait symmetry at baseline. In the following session (*weight*), the task was similar except for the addition of the ankle weight. Healthy individuals require approximately 50 strides to reach steady-state joint patterns after the addition of external weights. The deadadaptation process is usually slower, and can take up to 70 strides [28]. To guarantee a complete wash-out before testing the controller, we included a *deadadaptation* session that resembled the baseline. The last session (*force field*)

involved testing the effects of the adaptive force field on the subject walking with the weights. Besides haptic guidance, in this session participants were also given augmented visual feedback on the target footpath and on the current position of their foot.

Data collected by the robot in the last 60 seconds of each session were sampled at 500Hz and processed. Stride-to-stride subdivision was achieved by means of footswitches. In the following, we present results from two representative symmetry metrics, the *normalized error area* (NEA) and the *double-support ratio* (DS ratio), which address spatial and temporal asymmetry, respectively. The former was defined as the deviation area between two successive left and right footpaths, divided by the area of the reference footpath (right leg footpath). *t*-tests were run on each subject separately, to check for significant differences in the two metrics across the 4 sessions ($\alpha = 0.05$). Bonferroni's correction was utilized to control the familywise error rate.

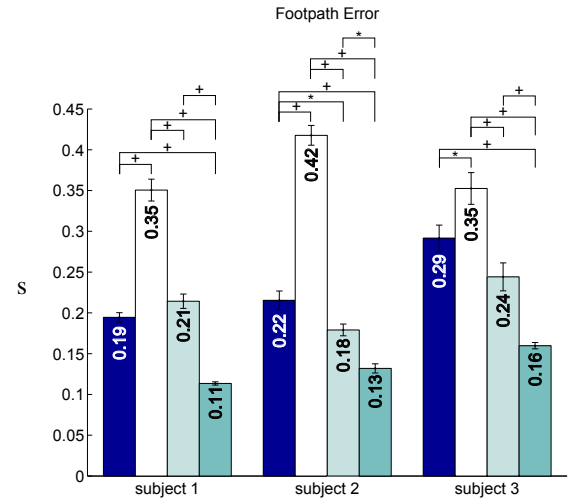
B. Results

1) *Spatial symmetry*: Fig. 6a shows that for all the subjects, the addition of the ankle weight significantly increased the deviation area between the left and right footpaths compared to *baseline* ($p < 0.001$). This result is in line with previous findings [28], [29], suggesting that loads $< 2\text{kg}$ attached to the lower extremities can alter gait kinematics significantly. The baseline value was successfully recovered during *deadaptation*.

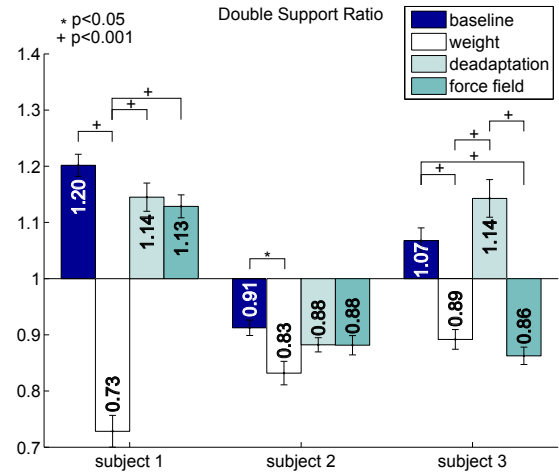
All three subjects were able to improve gait symmetry when walking with the adaptive controller, with the deviation area being significantly smaller than in the *weight* session ($p < 0.001$). An interesting result is that the deviation area was actually smaller than in the *baseline* session for all the subjects ($p < 0.001$). This might be due to the combined effect of haptic guidance and visual feedback, the latter favoring accurate volitional control of the foot trajectory.

In general, these results suggest that the locomotor control system of healthy subjects can take advantage of the assistance provided by the adaptive force field to successfully compensate for the disturbance caused by ankle weighting and recover a more symmetrical gait pattern.

2) *Temporal symmetry*: The double support ratio is the ratio between double support of the right leg and that of left leg. During double support, the weight is progressively transferred to either the left leg (right DS) or to the right leg (left DS). A DS ratio less than unity, then, indicates decreased time available to shift the load to the left leg. This change was significant in all three subjects, when comparing the *weight* session to *baseline* ($p < 0.001$, Fig. 6b). A known effect of asymmetric weighting is increased swing time in weighted limb due to the extra mass [30]. This was reflected in all subjects by a decrease in the ratio of the stance periods of right and left legs (not reported here for the sake of brevity). A prolonged swing period in the left leg, in turn, would delay the initial contact of the left foot, thus reducing the right DS. During the *deadaptation* session, this deviation was recovered



(a) Error area between the left and right footpath, normalized to the area of the right footpath (NEA).



(b) DS ratio (Right/Left) for each subject.

Fig. 6: Experimental results

by all subjects ($p > 0.05$). The adaptive force field helped subject 1 and 2 recover temporal symmetry, their DS ratio in session *force field* being not significantly different from the baseline value. This was not the case of subject 3 ($p = 0.004$), whose DS ratio during the last session was actually close to the non-assisted weighted condition ($p > 0.05$).

In summary, the force-field proved to be more effective in restoring spatial symmetry than temporal symmetry, at least for one subject. A possible explanation is that the force field prescribed a target *footpath* rather than a target *trajectory*, thus allowing subjects to adjust the actual timing of movement.

Yet, spatial and temporal variables were linked by the constraint on the walking speed (imposed by the treadmill), and this would explain the beneficial effects on temporal symmetry detected in subject 1 and 2.

V. CONCLUSION

This paper presented the overall design of ALEX III and a first application of the robotic platform, motivated by asymme-

tries typical of hemiparetic gait. The controller continuously modulates the force field applied to the impaired leg based on the outputs of kernel-based non-linear filters that learn the movements of the unimpaired leg, and can thereby smoothly accommodate changes in gait pattern and timing, such as those derived from modifying the walking speed.

Experimental results showed that the controller was effective in helping 3 healthy subjects improve gait symmetry, after their gait pattern was temporarily altered by ankle weights. Spatial symmetry was recovered more easily than temporal symmetry. It should be noted that our results - though promising - are only preliminary, and further tests need to be run on a larger sample size before drawing any general conclusion on the effectiveness of the controller on healthy subjects. Indeed, the controller improved subjects' spatial symmetry even beyond the baseline values: given the AAN nature of the force controller, we speculate that this effect was due to the visual feedback (active during the force field session) favoring accurate volitional control of the foot trajectory, rather than to the robot assistance. A modified experimental protocol including a session with haptic guidance only and one with visual guidance only would help confirm this hypothesis.

Finally, whether or not similar positive results would transfer to hemiparetic subjects is still an open question that can only be answered with future tests on clinical population.

VI. ACKNOWLEDGMENT

This work was supported by the National Institute of Health, Grant No. HD 38582.

REFERENCES

- [1] P. M. Kelly-Hayes *et al.*, "The american heart association stroke outcome classification," *Stroke*, vol. 29, no. 6, pp. 1274–1280, 1998.
- [2] C. Richards, F. Malouin, and C. Dean, "Gait in stroke: assessment and rehabilitation," *Clinics in geriatric medicine*, vol. 15, no. 4, pp. 833–855, 1999.
- [3] U.-B. Flansbjer, A. M. Holmback, D. Downham, C. Patten, and J. Lexell, "Reliability of gait performance tests in men and women with hemiparesis after stroke," *Journal of rehabilitation medicine*, vol. 37, no. 2, pp. 75–82, 2005.
- [4] H. S. Jørgensen, H. Nakayama, H. O. Raaschou, and T. S. Olsen, "Recovery of walking function in stroke patients: the copenhagen stroke study," *Archives of physical medicine and rehabilitation*, vol. 76, no. 1, pp. 27–32, 1995.
- [5] B. French *et al.*, "Repetitive task training for improving functional ability after stroke," *Stroke*, vol. 40, no. 4, pp. e98–e99, 2009.
- [6] R. P. Van Peppen, G. Kwakkel, S. Wood-Dauphinee, H. J. Hendriks, P. J. Van der Wees, and J. Dekker, "The impact of physical therapy on functional outcomes after stroke: what's the evidence?" *Clin Rehabil*, vol. 18, no. 8, pp. 833–862, Dec. 2004.
- [7] A.-L. Hsu, P.-F. Tang, and M.-H. Jan, "Analysis of impairments influencing gait velocity and asymmetry of hemiplegic patients after mild to moderate stroke," *Archives of physical medicine and rehabilitation*, vol. 84, no. 8, pp. 1185–1193, 2003.
- [8] K. K. Patterson, W. H. Gage, D. Brooks, S. E. Black, and W. E. McIlroy, "Evaluation of gait symmetry after stroke: a comparison of current methods and recommendations for standardization," *Gait & posture*, vol. 31, no. 2, pp. 241–246, 2010.
- [9] G. Rosati, "The place of robotics in post-stroke rehabilitation," *Expert Review of Medical Devices*, vol. 7, no. 6, pp. 753–758, 2010.
- [10] G. Colombo, M. Joerg, R. Schreier, V. Dietz *et al.*, "Treadmill training of paraplegic patients using a robotic orthosis," *Journal of rehabilitation research and development*, vol. 37, no. 6, pp. 693–700, 2000.
- [11] A. Pennycott, D. Wyss, H. Vallery, V. Klamroth-Marganska, R. Riener *et al.*, "Towards more effective robotic gait training for stroke rehabilitation: a review," *Journal of neuroengineering and rehabilitation*, vol. 9, no. 1, pp. 1–13, 2012.
- [12] V. S. Huang and J. W. Krakauer, "Robotic neurorehabilitation: a computational motor learning perspective," *Journal of NeuroEngineering and Rehabilitation*, vol. 6, no. 1, p. 5, 2009.
- [13] D. P. Ferris, G. S. Sawicki, and A. Domingo, "Powered lower limb orthoses for gait rehabilitation," *Topics in spinal cord injury rehabilitation*, vol. 11, no. 2, pp. 34–49, Jan. 2005.
- [14] D. J. Reinkensmeyer *et al.*, "Tools for understanding and optimizing robotic gait training," *Journal of rehabilitation research and development*, vol. 43, no. 5, p. 657, 2006.
- [15] D. J. Rutherford and C. Hubley-Kozey, "Explaining the hip adduction moment variability during gait: Implications for hip abductor strengthening," *Clinical Biomechanics*, vol. 24, no. 3, pp. 267–273, 2009.
- [16] R. R. Neptune, S. A. Kautz, and F. E. Zajac, "Contributions of the individual ankle plantar flexors to support, forward progression and swing initiation during walking," *Journal of biomechanics*, vol. 34, no. 11, pp. 1387–98, Nov. 2001.
- [17] S. K. Banala, S. H. Kim, S. K. Agrawal, and J. P. Scholz, "Robot assisted gait training with active leg exoskeleton (alex)," *Neural Systems and Rehabilitation Engineering, IEEE Transactions on*, vol. 17, no. 1, pp. 2–8, 2009.
- [18] P. Stegall, K. Winfree, D. Zanotto, and S. Agrawal, "Rehabilitation exoskeleton design: Exploring the effect of the anterior lunge degree of freedom," *Robotics, IEEE Transactions on*, vol. 29, no. 4, pp. 838–846, 2013.
- [19] L. Righetti, J. Buchli, and A. J. Ijspeert, "Dynamic hebbian learning in adaptive frequency oscillators," *Physica D: Nonlinear Phenomena*, vol. 216, no. 2, pp. 269–281, 2006.
- [20] A. Gams, A. J. Ijspeert, S. Schaal, and J. Lenarčič, "On-line learning and modulation of periodic movements with nonlinear dynamical systems," *Autonomous robots*, vol. 27, no. 1, pp. 3–23, 2009.
- [21] R. Ronsse, N. Vitiello, T. Lenzi, J. van den Kieboom, M. C. Carrozza, and A. J. Ijspeert, "Human-robot synchrony: flexible assistance using adaptive oscillators," *IEEE Transactions on Biomedical Engineering*, vol. 58, no. 4, pp. 1001–1012, 2011.
- [22] T. Lenzi, D. Zanotto, P. Stegall, M. Carrozza, and S. Agrawal, "Reducing muscle effort in walking through powered exoskeletons," in *2012 Annual International Conference of the IEEE Engineering in Medicine and Biology Society (EMBC)*, 2012, pp. 3926–3929.
- [23] W. van Dijk, H. van der Kooij, B. Koopman, and E. H. van Asseldonk, "Improving the transparency of a rehabilitation robot by exploiting the cyclic behaviour of walking," in *2013 IEEE International Conference on Rehabilitation Robotics (ICORR)*, 2013.
- [24] D. Zanotto, P. Stegall, and S. K. Agrawal, "ALEX III: a novel robotic platform for gait training, design the 4-dof leg," in *Proc. of the IEEE Int. Conf. on Robotics and Automaton ICRA2013*, 2013, sent for publication.
- [25] D. Reinkensmeyer, J. Wynne, and S. Harkema, "A robotic tool for studying locomotor adaptation and rehabilitation," in *24th International Conference of the IEEE Engineering in Medicine & Biology Society*, vol. 3, oct. 2002, pp. 2353 – 2354 vol.3.
- [26] J. Emken, J. Wynne, S. Harkema, and D. Reinkensmeyer, "A robotic device for manipulating human stepping," *IEEE Transactions on Robotics*, vol. 22, no. 1, pp. 185 – 189, feb. 2006.
- [27] D. Zanotto, P. Stegall, and S. K. Agrawal, "Improving transparency of powered exoskeletons using force/torque sensors on the supporting cuffs," in *2013 IEEE International Conference on Rehabilitation Robotics (ICORR)*, 2013.
- [28] J. W. Noble and S. D. Prentice, "Adaptation to unilateral change in lower limb mechanical properties during human walking," *Experimental brain research*, vol. 169, no. 4, pp. 482–495, 2006.
- [29] T. D. Royer, P. E. Martin *et al.*, "Manipulations of leg mass and moment of inertia: effects on energy cost of walking," *Med Sci Sports Exerc*, vol. 37, no. 4, pp. 649–56, 2005.
- [30] H. Skinner and R. Barrack, "Ankle weighting effect on gait in able-bodied adults," *Archives of physical medicine and rehabilitation*, vol. 71, no. 2, p. 112, 1990.